Experimental Study of Oil-Water Emulsions Injected into a Subsonic Crossflow

C.D. Bolszo, G.A. Gomez and V.G. McDonell[1*]
Department of Mechanical and Aerospace Engineering
University of California, Irvine
Irvine, CA 92697-3550 USA
cdb@ucicl.uci.edu and gag@ucicl.uci.edu

Abstract

The current study investigates the influence of introducing water and diesel fuel oil as an emulsion on the penetration of a liquid jet into a gaseous crossflow. Tests are conducted at atmospheric pressure, with momentum flux ratios spanning 30 – 120 with water addition of up to 40 percent. Liquid and gas velocities up to 20 and 80 m/s, respectively are considered. Nozzle Reynolds numbers ranged from 3,000 - 11,000 and aerodynamic Weber numbers spanned from 200 – 1,400. The spray morphology, in conjunction with edge filtering and intensity thresholding, was utilized to establish the spray plume edge. Existing liquid jet trajectory equation framework successfully correlates the penetration of the spray plume without modification to account for characteristics of emulsions. It is also observed that, for the conditions studied which span between column and shear mode breakup, the breakup mode itself also influences the ability of the correlations to describe penetration.

Introduction

In fuel preparation scenarios where high momentum air is available in large volumes, the breakup of liquid in a subsonic crossflow is most commonly achieved by ejecting a column of liquid as a jet, perpendicularly (or angles near to) into a gaseous air flow. This strategy has been utilized for various applications including rocket propulsion, turbofan, turbojet, ramjet, scramjet engines/afterburners and power generation by industrial gas turbines. Therefore, it is of interest to understand the breakup, atomization and trajectory of the energy carrying fluid to control the heat release and combustion chemistry. This subject has been studied for several decades [1-16]. Progress on understanding this injection strategy involves investigating and modeling the liquid breakup and plume structure. Studies that elucidated the governing physics provided a means for predicting the overall spray shape utilizing physical-empirical correlations [3,4] Equations have proposed different forms of influencing variables, grouping of variables and to varying degrees of influence [5,6].

As liquid is introduced perpendicularly into a gaseous crossflow, interaction of the fluid streams occurs. Figure 1 (due to Wu et. al (1997)) illustrates a representative visual schematic of the main breakup processes.

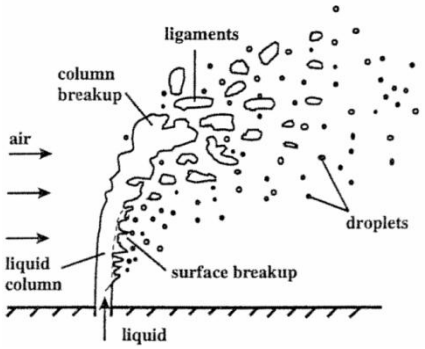

Figure 1 Representative schematic of jet-in-Crossflow [5]

Considering applications where a water source is readily available alongside fuel oil, these two liquids can be combined to improve atomization when prepared as an emulsion [17, 18]. A water-in-oil emulsion's component liquids can be introduced at a T-junction, to be further mixed and finally atomized. Application of the current injection strategy has merit in the fuel preparation of liquid fueled combustion systems. In studying the current jet-in-crossflow injection strategy and fuel stream availability is of current interest in order to improve system efficiency in large scale industrial gas turbine systems for power generation.

The liquid begins to deform, then breakup and mix with the crossflow stream. The momentum interaction of both fluids breakup the jet and the gas flow then carries the liquid downstream from the initial point of injection

* Corresponding author: mcdonell@ucicl.uci.edu

along a wall. The liquid undergoes a transfer of momentum in the crossflow, resulting in a downstream liquid trajectory as it penetrates into the gaseous flow. Surface breakup occurs as gas momentum interactions at the liquid surface, flatting the column shape from circular into an ellipse and stripping droplets off of the column [7]. Column breakup occurs as the liquid trajectory encounters the gas stream, bending with the crossflow streamlines and along its surface a Kevin-Helmholtz type instability develops [8,9]. As the instability grows, the column eventually pinches off a parcel of fluid which forms into a ligaments and then droplets. Droplets are also being sheared off the column as the liquid deforms along its trajectory. These droplets can undergo further deformation and secondary atomization as well [10, 11].

To compare the force contribution to the resulting liquid breakup is the momentum flux ratio (q), Equation 1), which is the ratio of the liquid to the gaseous crossflow momentum flux, where ρ and U are density and mean velocity of the liquid and gaseous streams.

$$\mathrm{q} = \frac{\rho_l U_l^2}{\rho_g U_g^2} \tag{1}$$

More recent work attributes aerodynamic Weber Number (W_{aero}), defined in Equation (2, to jet breakup modes in the crossflow at both atmospheric [14] as well as at elevated pressure conditions [12]. W_{aero} considers the incompressible air density (ρ_g), the mean crossflow velocity (U_g), the nozzle diameter (d) and the liquid surface tension (σ), and droplet histograms/velocities.

$$We_{areo} = \frac{\rho_g U_g^2 d}{\sigma} \tag{2}$$

Refined and validated modeling approaches of jet column breakup, penetration and atomization in a crossflow have evolved as a result of the aforementioned experimental studies and analyses [6]. The evolution of high speed visualization has led to better understanding of the breakup of jets-in-cross flow [e.g., 13]. The visualization of the breakup process has allowed for "validation" of advanced numerical simulations of the primary breakup modes [e.g., 9].

In terms of emulsions, as a first step, it is of interest to assess the extent to which more simplified correlations, derived for homogeneous liquids, can describe basic spray plume parameters such as penetration. Many specific penetration equations have been developed by different groups under different experimental conditions. The early correlation presented by Wu and coworkers (1998) [5] is a simple dimensionless relation that includes the momentum flux ratio, nozzle diameter and downstream distance (x) to predict the penetration height (y) and is shown in Equation 3. The data used to develop this correlation featured values of q from 5 to 50. Hassa and co-workers [6] provided a slightly modified version using data at elevated pressure with q varying from 1-40, provided as Equation 4. Additional correlations by Stenzler et al. (2003) [14] and Birouk et al. (2007) [15] included the effect of We_{aero} and viscosity on trajectory predictions, which forms are represented in Equations 5 and 6. Work by Lee et al. (2007) [16] investigated the penetration of round turbulent jets in a crossflow over a large range of q from 3-200 and included the liquid column drag coefficient (C_D) as shown in Equation 7, which was set to a constant value of 3 for shear breakup.

$$\frac{y}{d} = aq^{\mathrm{b}} \left(\frac{x}{d}\right)^c \tag{3}$$

$$\frac{y}{d} = aq^{\mathrm{b}} \ln\left(1 + \mathrm{c}\left(\frac{\mathrm{x}}{\mathrm{d}}\right)\right) \tag{4}$$

$$\frac{y}{d} = aq^b \left(\frac{x}{d}\right)^c We^e \left(\frac{\mu_l}{\mu_w}\right)^f \tag{5}$$

$$\frac{y}{d} = aq^b \left(\frac{x}{d}\right)^c \left(\frac{\mu_l}{\mu_w}\right)^e \tag{6}$$

$$\left(\frac{y}{dq}\right) = \sqrt{\pi/C_D} \left(\frac{x}{dq}\right)^a \tag{7}$$

Objective and Approach

The objective of the present study is to ascertain the degree to which an emulsion penetrates in a manner which can be described by existing correlations that have been developed for homogeneous liquids. To assess this, high speed imaging of the behaviour of liquid jets of emulsions with varying characteristics is carried out and the resulting images analysed for penetration tendencies which are compared to those predicted by previously developed correlations.

Experimental Methods

The jet-in-crossflow experiment was conducted on an atmospheric spray test stand. A straight, rectangular test section was used; with dimensions of 101.6 mm (height; y-dir) x 355.6 mm (length; x-dir) x 76.2 mm (width; z-dir). The liquid jet nozzle exits were flush with the test section wall. A photo with data and coordinate axes overlaid is provided in Figure 2a. The crossflow air enters from the left of the test section, which is established to be in line with the x-direction. A cylindrical air box provides a large volume to expand and straighten the air stream through grid meshes, initially exiting from a 50.4 mm pipe, which is situated upstream of the test section (displayed in a vertical orientation in Figure 2b). The experimental test section and air box are coupled by a circular to rectangular transition piece. Air flow is metered using a critical flow orifice with parallel coarse and fine needle valves and a precision pressure gauge (Figure 2c). The air flows through a flexible line to the top of the test section, which is all mounted on top of a three axis traverse.

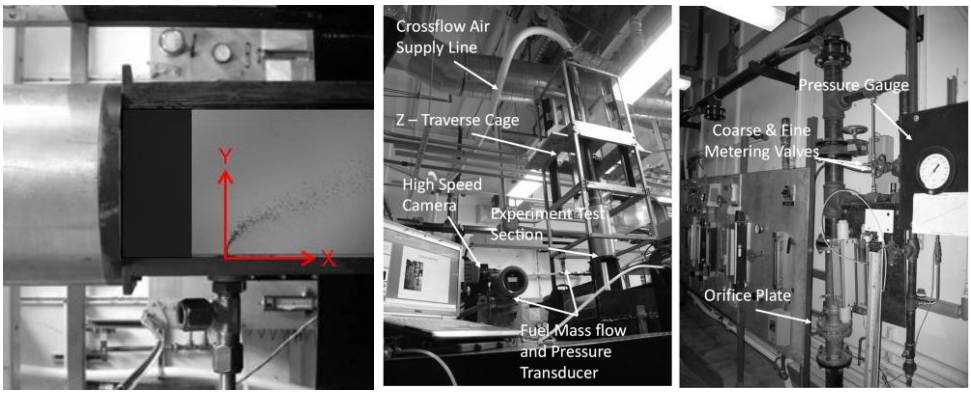

Figure 2 Spray in crossflow experiment showcasing a) test section, b) test rig setup & c) crossflow air setup

The nozzle geometry allowed for fully developed flow to develop upstream of the exit plane. A liquid flow length (L) of 8mm with a sharp edged entrance was used. Two nozzle diameters (d), 0.57 and 0.72 mm, equating to L/d values of 14.0 and 11.1, respectively were used in the testing.

The liquids used in this study are low sulfur distillate #2 (DF2) and filtered water from the tap. The measured fluid properties these test liquids are provided in Table 1. Surfactants were not used. Rather, emulsions were generated with a low pressure drop (~1psi) static mesh mixer following the introduction of each component into a T-junction. The resulting emulsion then flows ~25 cm to the point of injection. To prevent possible coalescence, a second screen filter was placed 3 mm prior to the final contraction into the orifice nozzle or 11mm from the nozzle exit plane. Discrete water droplet distributions were determined to be in the low limit of macro-emulsions (1 to 30 μm range) based on experiments comparing performance from stabilized emulsions and unstable emulsions [17,18].

Table 1 Liquid properties (laboratory ambient conditions)

	DF2	**Water**
Chemical Formula	$C_{10\text{-}14}H_{20\text{-}28}$	H_2O
Density (ρ_l) [kg/m^3]	825	1012
Viscosity (μ_l) [kg/m-s]	2.93E-03	1.37E-03
Surface Tension (σ) [kg/s^2]	0.0280	0.0693

Three water mass fractions (Φ) were selected: neat DF2 Φ=0.00, emulsion with Φ=0.23 and an emulsion with Φ=0.38. A single liquid flow rates were chosen for each nozzle in order to isolate the influence of the effect of an emulsion on the emulsion plume. Crossflow air flow rate was varied between three values, with the average profile velocity used from calculation. The tabulation of the test values utilized in the current work is presented in Table 2.

High speed cinematography (Vision Research Phantom 7.2 camera) was utilized to capture videos for jet-in-cross flow experiments of unstable emulsions. A 2 μs exposure rate at was utilized for each frame. The video captured for each case was trimmed to 300 frames sampled from the full frame rate cine file at a rate of 20 frames per second to ensure effective time averaging. A Sobel operator which isolates the largest directional gradient from light to dark pixels, allowing emphasis of the edge was selected as most effective in edge distinction. This filter operation was applied to each video and was performed within the Phantom Camera Control software. Penetration was then based on the resulting top edge of the spray plume. The gradient vector edge was identified by computing the intensity derivative and the values in vertical direction were used, any region of constant intensity values was nulled, a procedure described and outlined in image processing texts [19].

Table 2 Conditions for jet-in-crossflow test matrix

Nozzle Diameter (d) [mm]	0.57			0.72		
Crossflow Air Velocity, (U_g) [m/s]	44	52	68	44	52	68
Crossflow Mass Flow [kg/min]	24	29	38	24	29	38
Liquid Velocity (U_l) [m/s]	14			18		
Liquid Inject. Pressure (ΔP_l) [MPa]	0.086			0.124		
Liquid Mass Flow [kg/min]	0.12			0.25		
Emulsion Water Mass Fraction (Φ)	0.00	0.23	0.38	0.00	0.23	0.38
Comparison Momentum Flux Ratio (q)	27	46	60	44	82	117
Nozzle Reynolds Number ( )	4,000 – 11,000			3,000 – 8,000		
Aerodynamic Weber Number ( )	300 – 1,400			300 -1,100		

After the edge Sobel vertical filter is applied, each frame in the video is further processed using MATLAB to filter out any noise and interferences that are not associated with the spray plume. This is accomplished by initially converting the frame into a binary image. The MATLAB function for conversion to binary requires the input of a cut-off intensity value (LEVEL), from which pixels of grayscale intensity (0-1) above the chosen value will be accepted and converted. It is difficult to assign a constant LEVEL value for all cases since the variation in liquid/water concentration obscuring the backlighting will affect the light luminosity for each image. As a result, a different LEVEL value must be applied to each frame. The LEVEL value is chosen using MATRIX's GRAYTHRESH function, which implements Otsu's method to determine the cut-off intensity value. Otsu's method classifies the pixels into either foreground or background pixels and calculates the optimal threshold value that separates the two classifications. This is the then the threshold value used in place of LEVEL. Once 300 frames are converted to binary images, they are time averaged into one image, as Figure 3a displays.

To capture the penetration into the crossflow, the top edge of the spray plume was trace. A MATLAB code was developed to trace the pixels with the highest y coordinate value for every x coordinate, mapping the pixels on a y vs. x plot. In order for the code to trace the top edge of the plume, the image is converted to binary again so that all pixels regardless of value are given a value of unity. This allows the code to simply trace the pixels with the highest y coordinate using a programming loop, as displayed in Figure 3b.

Figure 3 a) Time averaged image, b) binary image of emulsion case with Φ=0.23, q=52 & c) trace of morphology processed plume

A few white pixels or regions of pixels (attributed to rouge droplets, noise or instrument error) are noted away from the main spray plume represent outlying or non-physical features in the trajectory. Although these points demonstrate that liquid droplets exist outside of the spray plume area, they interfere with the desired smooth trace of the plume edge as shown in Figure 3c. To mitigate interference by these white pixels, MATLAB's "BWAREAOPEN" function was utilized. This function removes clusters of pixels that are connected in groups of less than a given integer. An integer value of 200 was visually determined as a sufficient value to distinguish between unnecessary pixels and isolate the dominant morphology in the trajectory arch. Application of this function removes the unwanted spots from Figure 3a, but does not remove any connected features, which defines the boundary of interest for the trace, and demonstrated in Figure 3b. The boundary determined binary fields, which have been treated for enhanced upper edge detection intensity and morphology thresholding, are now traced on the top surface along every x pixel. Distinguished by the darkened traced line on the spray boundary and was utilized as a representative trajectory for each jet-in-crossflow test case and further penetration analysis in Figure 3c.

Results

Discharge Coefficients and Breakup Regimes

The orifice nozzle discharge coefficient (C_d) for the two nozzles, defined in Equation (8, was measured for over the laminar to fully turbulent range at a given nozzle Reynolds number (Re_N), defined in Equation (9. The results are provided in Figure 4. In the current test, Re_N varied from 1,500 to 3,000 for neat DF2 (Φ=0.00), which corresponds to an injector C_d varying from 0.65 to 0.70 for the 0.72 and 0.57mm diameter nozzles.

$$C_d = \frac{\dot{m}_l}{A_o\sqrt{2\rho_l \Delta P_l}} \tag{8}$$

$$Re_N = \frac{\rho_l U_l d}{\mu_l} \tag{9}$$

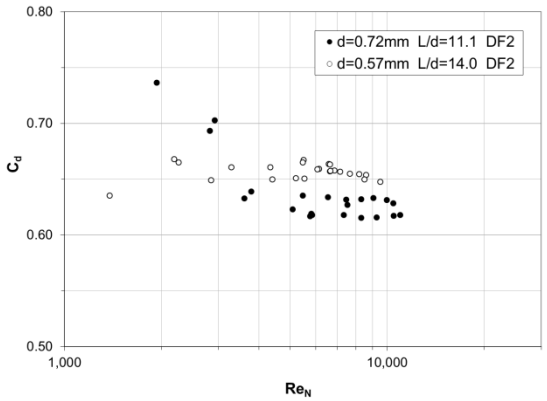

Figure 4 C_d vs. Re_N from laminar to turbulent flow

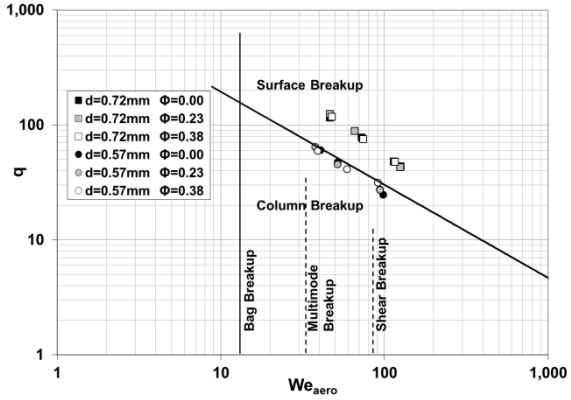

Figure 5 q vs. We_{aero} regime plot for current test cases.

To establish the expected breakup mode for the conditions studied, the current test cases are plotted on a q versus We_{aero} regime map [5] in Figure 5. Figure 5 indicates a difference in dominant breakup behavior between the neat and emulsion cases. The difference between the two regimes (resulting from use of emulsion vs neat liquids) can also be observed in images as illustrated in Table 3.

Table 3 Single high speed exposure of DF2 and emulsions

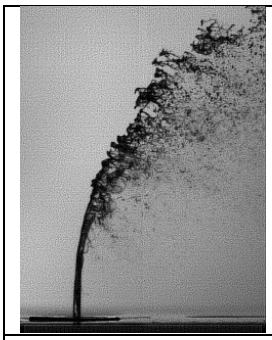	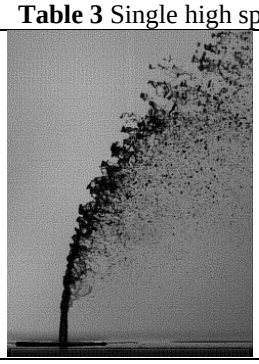	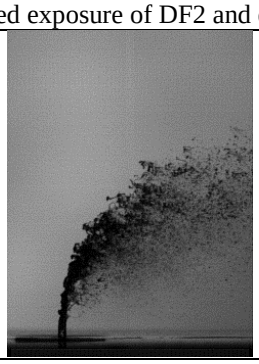	
D=0.72mm q=116 Φ=0.00	**D=0.72mm q=118 Φ=0.38**	**D=0.72mm q=44 Φ=0.00**	**D=0.72mm q=48 Φ=0.39**
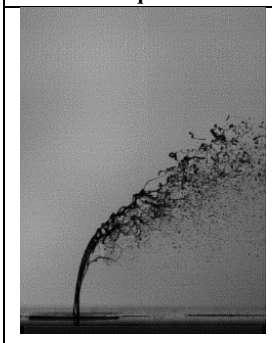	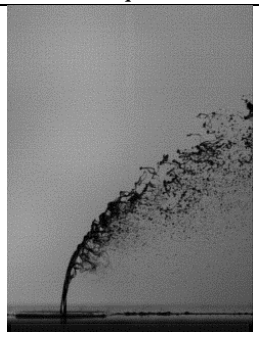	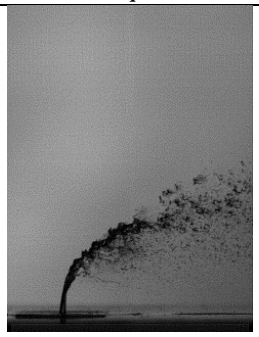	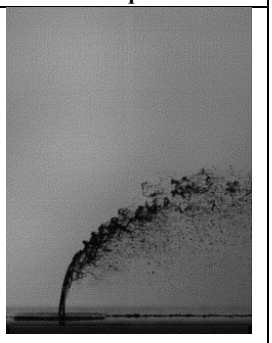
D=0.57mm q=60 Φ=0.00	**D=0.57mm q=59 Φ=0.38**	**D=0.57mm q=25 Φ=0.00**	**D=0.57mm q=32 Φ=0.34**

As shown in Table 3, larger numbers of droplets are produced from surface stripping at higher versus lower momentum flux ratios. However, it is also observed that less fine droplets are produced when significant amounts of water are added to form an emulsion (varying Φ) for a given case, consistent with the different regimes suggested by Figure 5.

Penetration Behavior

Resultant edge enhanced average averaged exposures utilizing 300 images in comparison to one 2μs exposure is provided in a side-by-side comparison in Figure 6. In comparing all of the averaged cases, the difference between the intensity was of prime interest in assessing a representative exposure for line boundary determination in distinguishing from backlighting or background intensity gradients.

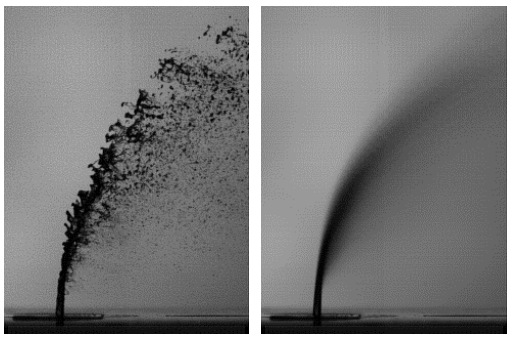

Figure 6 a) High speed exposure & b) example 300 exposure average of test case used for determining plume trajectory (d=0.57mm q=46 Φ=0.24)

The methodology described above was used to establish the plume trajectory. Table 4 summarizes the average intensity cutoff value in distinguishing between a black (0) and white (1) pixel color (value) in binary. Also provided is the standard deviation in averaged lighting value in determining the intensity threshold for 300 exposures. With the exception of one case at d=0.72, Φ=0.00 and q=44, the average threshold intensity was consistently very near 0.3 and a standard deviation of 0.01.

Table 4 Intensity threshold values from Otsu's method

Flow Conditions			Intensity Threshold		Flow Conditions			Intensity Threshold	
d (mm)	Φ (0 - 1)	q ( )	Ave. (0 - 1)	StDev. (0 - 1)	d (mm)	Φ (0 - 1)	q ( )	Ave. (0 - 1)	StDev. (0 - 1)
0.72	0.00	116	0.290	0.011	0.57	0.00	60	0.331	0.007
0.72	0.22	125	0.298	0.012	0.57	0.23	65	0.316	0.007
0.72	0.38	118	0.290	0.011	0.57	0.38	59	0.325	0.009
0.72	0.00	78	0.272	0.011	0.57	0.00	47	0.299	0.009
0.72	0.22	88	0.281	0.012	0.57	0.24	46	0.280	0.008
0.72	0.36	75	0.272	0.011	0.57	0.38	41	0.296	0.008
0.72	0.00	48	0.246	0.015	0.57	0.00	25	0.243	0.014
0.72	0.00	44	0.182	0.016	0.57	0.22	27	0.252	0.014
0.72	0.24	43	0.248	0.015	0.57	0.22	27	0.243	0.015
0.72	0.39	48	0.257	0.014	0.57	0.34	32	0.254	0.011

The trajectories from the processed images of neat DF2 for three general q's are provided in Figure 7. For each case, the trajectory is monotonically increasing with q (increase in liquid versus gas) except for the 0.72 mm diameter, q = 116 case which has a trajectory close to the higher air flow case with q = 78.

Figure 8 presents the trajectories for the emulsions. The trend in trajectory for a given Φ (e.g., ~0.23 or ~0.38) suggests a strong direct proportionality with momentum flux ratio a given nozzle diameter. Yet for a given momentum flux ratio, no clear dependency on Φ is observed.

As a first step in evaluating applicability of prior correlations, analysis was carried out for neat DF2 (Φ=0.00). Equations 3 - 7 were considered. Of the correlations considered, the basic form presented by Wu and coworkers (Equation 3) provided consistently the best fit to the current data set. The goodness-of-fit is displayed as a linear least squares regression fit R^2 value and slope in Figure 9. One question to consider is whether the discharge coefficient the orifices contibutes to variation. A C_d=1.0 was used in Figure 9, as implemented in the original work [5]. The best fit coefficients were a=2.81, b=0.382 and c=0.374. Work by Brown et al [20] demonstrated the collapse of multiple jet-in-crossflow data sets are possible when considering the nozzle effective area by incorporating the C_d. Including the Cd effect on jet velocity (and thus q) does provide an

improvement in the correlation for each case, shown in Figure 10. This improved fit, demonstrated by an improved R^2 from 0.9179 to 0.9365 for DF2. The C_d did not vary substantially among the cases, but including it improves the correlation. The coefficients that provided this best fit were a=2.04, b=0.384 and c=0.385 and the full form is provided in Equation 10. While the C_d between the cases did not vary substantially, inclusion of the C_d results in a substantial increase in q which illustrates the need to clearly specify the basis for the values of q used (i.e, based on C_d = 1 or actual C_d)

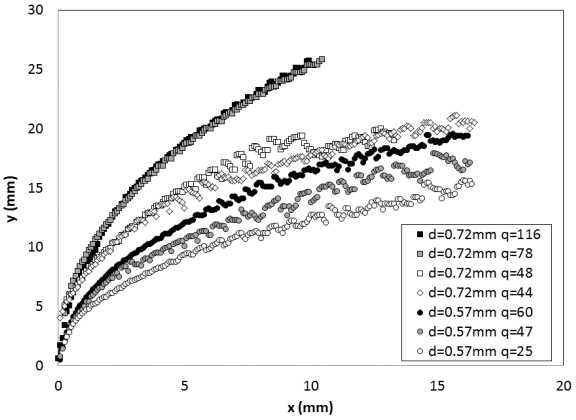

Figure 7 DF2 spray plume trajectory for two 0.57 & 0.72 mm orifices

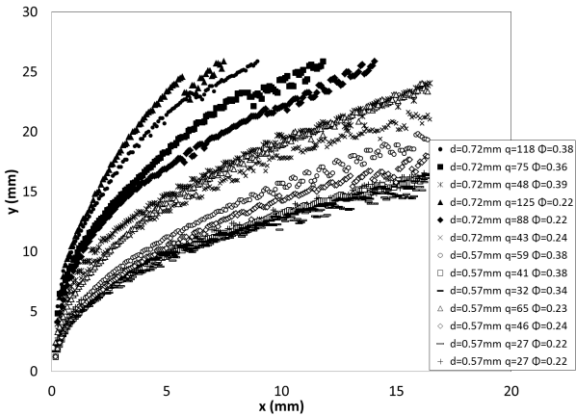

Figure 8 Emulsion spray plume trajectory for two 0.57 & 0.72 mm orifices

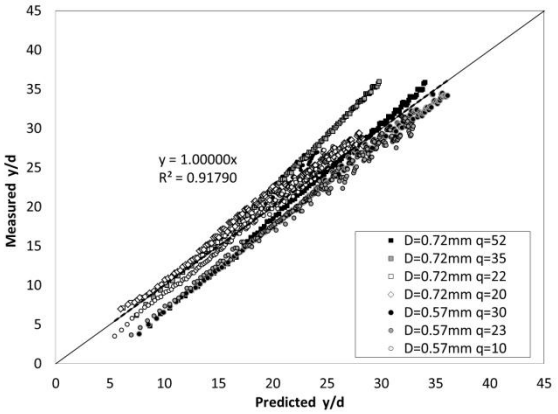

Figure 9 Spray plume edge trajectory measured vs. general correlation (Cd=1) for DF2

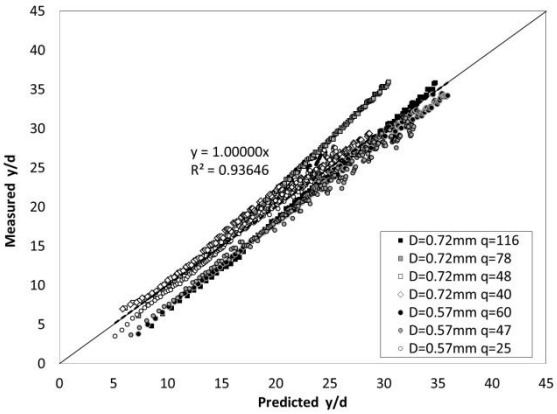

Figure 10 Spray plume edge trajectory measured vs. general correlation for DF2 C_d= 0.65– 0.70

$$\frac{y}{d} = 2.04q^{0.384}\left(\frac{x}{d}\right)^{0.385} \tag{10}$$

In further consideration of previous correlations, the effect of We_{aero} (Equation 5), Re_N and liquid viscosity (Equation 6), were all evaluated in the present work and were not found to demonstrate significant improvement in overall predictive fit. Refering to the work of Stenzler et al (2003) [14], an increase in the crossflow We_{Aero} intensifies the stripping of liquid from the surface and widens the spray dispersion. This results in finer droplet sizes downstream for the neat cases. For emulsions, the largest droplets appear to be those composed of higher concentrations of water. For the current emulsion, DF2 is the continuous phase and, due to (1) its greater chance to be at the gaseous interface upon injection and (2) its lower surface tension, will result in the formation of DF2 droplets or droplets with higher concentrations of DF2 stripped from the surface of the jet in the vicinity near the nozzle exit. Discrete water droplets within the emulsion, with higher density compared to DF2, will penetrate farther into the crossflow. If DF2 is shielding discrete water droplets from rupturing along their trajectory, they will experience less influence or disturbance from the crossflow, allowing larger, higher concentrated water droplets, to persist and penetrate farther into the crossflow. If this hypothesis regarding the detailed structure of the emulsion is correct, We_{aero} should result in less of an influence for emulsions versus the neat continuous component, DF2. Note that Stenzler reports only a minor influence of We_{aero} in the trajectory (exponent of -0.088 in Equation 5).

Considering both injectors, nozzle Reynolds numbers varied from laminar to turbulent (3,000 – 11,000). Figure 4 provided an assessment of discharge with regard to flow for neat DF2. For moderate to high Reynolds number cases, the Cd remained constant, however at much lower values, an increase is observed. Due to emulsions having higher viscosity than neat fuels the Cd will in turn correspond to a lower Reynolds number as was shown previously by the authors [18]. At Reynolds numbers near and above 10,000, cavitation was observed for the current nozzles, which, at times was violent enough to disrubt the majority of the jet core. For the given range tested, statistical regression did not find the the Reyonlds number (or Discharge Coefficient to have a significant effect on the spray trajectory. This may not be the case outside the range studied.

Of particular interest when considering emulsions was the increased viscosities and interfacial tension due to additional intermolecular forces present [17]. However, this viscosity effect was not shown to significantly impact the emulsion trajectory, converging towards low exponent values near 0.007. It was observed that the breakup length of the collumn occurred closer to the nozzle exit for the emulsions, however the viscoity, represented as a ratio of liquid to water viscosity in Eqs. 5 & 6, did not isolate this additional effect in producing an improved fit as an extra multiple in the basic correlation (Eq.3). An assessment of the surface to interfacial forces was conducted as well during the current analysis, and is currently ongoing.

To further isolate the relative behavior of emulsions and neat liquids, results for the combined results (neat and emulsions) were compared with the results for emulsions alone in Figures 11 and 12, respectively. Interestingly, including the emulsion cases did not degrade the regression fit, which maintianed a unity slope and a R^2=0.94. The trend in increasing trajectory with increasing Φ presented in Figure 8 is thus sufficiently accounted for by the increase in density from the water addition in within the DF2 for the emulsion. Past analyses have identified that the emulsion's fluid properties which are presently considered can be reprented as deviations from Newtonian flow behavior, which can be quantified as deviations from neat values of the continuous liquid (DF2) [17].

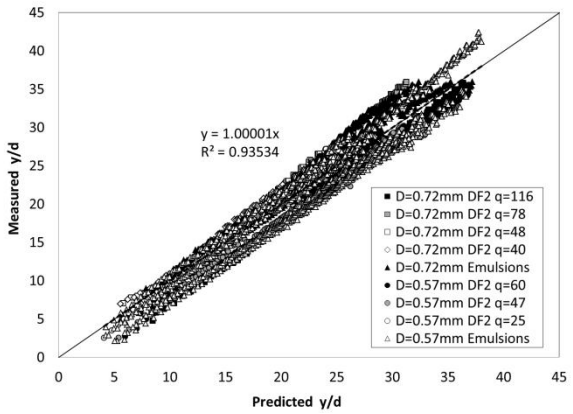

Figure 11 Spray trajectory edge measured vs. general correlation (C_d=0.65–0.70) for DF2 & Emulsions

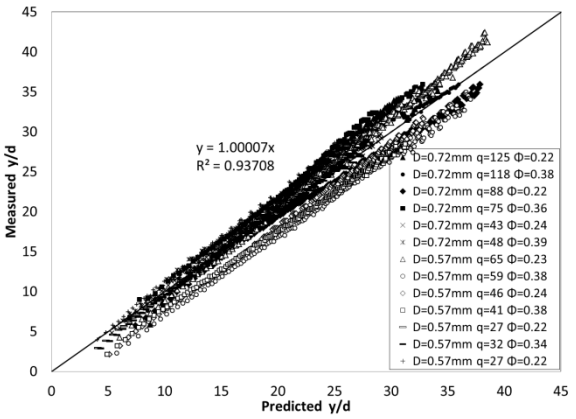

Figure 12 Spray trajectory edge measured vs. corrected general correlation (C_d=0.65–0.70) for Emulsions

Examining the coefficient values for b=0.384 and c=0.385 in Equation 10, it is evident that the eqution can be simplified to single exponent of 0.38 without any significant loss of fit, resulting in Equation 11:

$$\frac{y}{d} = 2.0\left(q\frac{x}{d}\right)^{0.38} \tag{11}$$

Finally, careful inspection of the results shown in Figures 7-12 does suggest some classification as a function of injector diameter. However, recalling that that the two injector diameters result in differing dominant breakup regimes (Figure 5), it is hypothesized that the variation in penetration due to injector diameter is due to the role of breakup regime. This suggests that different penetration correlations for different regimes may further improve the fit to the current data. However, from an engineering perspective, the improvement may not be substantial.

Summary and Conclusions

The penetration of liquid jets of unstable emulsions into a crossflow was investigated and reported, as to the best of the author's knowledge, for the first time. Experiments were carried out at atmospheric conditions for neat diesel fuel, two emulsion concentrations and three crossflow air flow rates. Two nozzle diameters were investigated. Results show that the penetration of emulsions, for the present conditions, can be predicted by simple versions of well-established correlations by Wu and coworkers [5] As a result, the influence of emulsification on the trajectory of is predominantly dictated by the modification in emulsion density, without the significant influence of interfacial forces. Apparent deviations in fit observed between the two injector diameters are attributed

to differences in the dominant breakup mechanisms (column vs shear) for each.

Acknowledgements

Siemens Energy partially supported this work.

References

[1] Leong, M.Y, (2000) Mixing of an airblast-atomized fuel spray injected into a crossflow of air, Ph.D. Thesis, University of California, Irvine.

[2] Leong, M.Y, McDonell, V.G., & Samuelsen, G.S. (2001) "Effect of ambient pressure on an airblast spray injected into a crossflow, *J. Propulsion and Power*, Vol. 17, No. 5,Sept.- Oct.

[3] Adelberg, M., (1967), "Breakup rate and penetration of a liquid jet in a gas stream," AIAA J., Vol. 5, No. 8, pp. 1408-1415.

[4] Schetz, J.A & Padhye, A. (1977) Penetration and breakup of liquids in subsonic airstreams, *AIAA Journal*, Nol. 15, NO. 10, pp. 1385 – 1390.

[5] Wu, P, Kirkendall, K.A., Fuller, R.P., & Nejad, A.S., (1998) "Spray structure of liquid jets atomized in subsonic crossflows," *J. Propulsion and Power*, Vol. 14, No. 2, pp 173-182.

[6] Rachner, M., Becker, J., Hassa, C., & Doerr, T., (2002) "Modeling of the atomization of a plain liquid fuel jet in crossflow at gas turbine conditions, *Aerospace Science & Technology*, 6, pp 495–506.

[7] Clark, B.J., (1964) Breakup of a liquid jet in a transverse flow of gas, NASA TN D-2424.

[8] Wu, P, Kirkendall, K.A., Fuller, R.P., & Nejad, A.S., (1998) "Breakup process of liquid jets in subsonic crossflows," *J. Propulsion and Power*, Vol. 13, No. 1, pp 64-73

[9] Herrmann, M. (2010) "Detailed numerical simulations of the primary atomization of a turbulent liquid jet in crossflow." *J. Eng. Gas Turbines & Power*, June. Vol. 132, 061506 1-10.

[10] Hinze, J.O. (1955) "Fundamentals of hydrodynamic mechanisms of splitting in dispersion processes," AIChE Journal, Vo. 1, No. 3, pp. 289 -295.

[11] Krzeczkowski, S.A. (1980) "Measurement of liquid droplet disintegration mechanisms," *International J. Multiphase Flow*, Vol. 6, No.3, pp.227-239.

[12] Lubarsky, E., Reichel, J.R., Zinn, B.T. & McAmis, R., (2010) "Spray in crossflow: dependence on Weber Number," *J. of Eng. for Gas Turbines and Power*. Feb.,Vol. 132, 021501-1 – 9.

[13] Brown, C. T., and McDonell, V. G., (2006) "Near field behavior of a liquid jet in a crossflow," ILASS Americas 19th Annual Conference on Liquid Atomization and Spray Systems.

[14] Stenzler, J.N., Lee, J.G, & Santavicca, D.A. (2003) Penetration of liquid jets in a crossflow, AIAA, Aerospace Sciences Meeting & Exhibit, Paper: 2003-1327 Reno NV.

[15] Birouk, M., Iyogun, C.O. & Popplewell, N. (2007) "Role of viscosity of trajectory of liquid jets in a cross-airflow, *Atomization & Sprays*, 17, pp 267-287.

[16] Lee, K, Aalburg, C., Diez, F.J., Faeth, G.M., & Sallam, K.A. (2007) "Primary breakup of turbulent round liquid jets in uniform crossflows, AIAA J., Vol. 45. No. 8.

[17] Bolszo, C.D., (2011) Pressure atomization of water-in-oil emulsions and the effect of gaseous crossflow, Ph.D. Dissertation, University of California, Irvine,

[18] Bolszo, C.D., Narvaez, A.A., McDonell, V.G., Dunn-Rankin, D. and Sirignano, W.A. (2010a) "Pressure-swirl atomization of water-in-oil emulsions." *Atomization and Sprays* 20(12):1077–1099.

[19] Gonzalez, R. C., Woods, R. E., & Eddins, S. L. (2004). *Digital Image Processing Using Matlab*. Upper Saddle River, NJ: Pearson Prentice Hall.

[20] Brown, C.T., Mondragon, U.M., and McDonell, V.G. (2007). Effect of nozzle discharge coefficient on penetration of a plain liquid jet injected into a crossflow. Presented at ILASS-Americas 2007, Chicago, Ill, May.